Vol. 33 (2002) *ACTA PHYSICA POLONICA B* No 10

CHARM FRAGMENTATION AND DIJET ANGULAR DISTRIBUTIONS*

Sanjay Padhi

On behalf of the ZEUS Collaboration

Department of Physics, McGill University, Montreal
Quebec, Canada, H3A 2T8
e-mail: spadhi@mail.desy.de

(Received July 5, 2002)

Charm fragmentation and dijet angular distributions have been measured in D^* photoproduction at HERA. Charm fragmentation and its property of universality is evaluated in terms of measurement of P_v, the ratio of vector/(vector + pseudoscalar) mesons. Angular distributions of dijets, with at least one of the jets associated with a $D^{*\pm}$ meson, have been measured for samples enriched in direct or resolved photon events. The differential cross section shows a steep rise for resolved events in the photon direction, providing strong evidence that the bulk of the resolved photon cross section is due to the charm content of the photon. The shallower rise for direct events as well as for resolved photon events in the proton direction are consistent with the quark exchange diagrams.

PACS numbers: 13.60.Le, 14.65.Dw

1. Introduction

Heavy quark photoproduction and fragmentation at HERA offers a novel way of testing both perturbative and non-perturbative aspects of quantum chromodynamics (QCD). In this paper parton dynamics (in terms of angular distributions) and fragmentation will be addressed based on recent ZEUS measurements.

* Presented at the X International Workshop on Deep Inelastic Scattering (DIS2002) Cracow, Poland, 30 April–4 May, 2002.

2. Charm fragmentation

A non-perturbative aspect of QCD can be measured by considering the spin dependence in fragmentation, which should in principle be sensitive to non-perturbative effects in the hadronisation process. ZEUS recently measured the fragmentation ratio P_v, ratio of vector/(vector + pseudoscalar). The value P_v can be calculated with respect to the ground-state charm mesons via the decay channels $D^{*+} \rightarrow D^0\pi_s^+ \rightarrow (K^-\pi^+)\pi_s^+(+\text{c.c.})$ and $D^0 \rightarrow K^-\pi^+(+\text{c.c.})$.

In this paper, the analysis [1] is based on $D^{*\pm}$ and D^0 events with an almost real photon (virtuality, $Q^2_{\text{median}} \sim 3.10^{-4}$ GeV^2) in a photon-proton center-of-mass energy, W, in the range $130 < W < 295$ GeV. Using $\triangle M = M(D*) - M(D^0)$ as a D^* tag, the sample is then further divided into D^0 mesons arising from and not from D^* mesons. After this division there were 1180 ± 39 events with a D^0 meson from a D^* and 5223 ± 185 inclusive D^0 meson events and the resulting value for P_v in the full phase space is:

$$P_v = 0.546 \pm 0.045(\text{stat.})^{+0.028}_{-0.028}(\text{syst.})\,.$$

This is in good agreement with the values of 0.57 ± 0.05 and 0.595 ± 0.045 [2] measured in e^+e^- annihilation.

3. Dijet in charm photoproduction

The angular distribution of outgoing partons in a hard partonic process is an efficient tool to study the parton dynamics of the underlying sub-processes. In leading order (LO) QCD these underlying sub-processes (Fig. 1) can be divided into either direct photon or resolved photon processes. In direct photon processes the photon participates in the hard scatter predominantly via the boson-gluon fusion process. This process has a quark as the propagator in the hard interaction. In resolved photon processes the photon acts like a source of incoming partons (quarks and gluons) and only a fraction of its momentum participates in the hard scatter. In this case both quark and gluon propagators are possible.

In order to probe the charm dynamics in these sub-processes and in particular to study the charm content of the photon, the following measurements have been made.

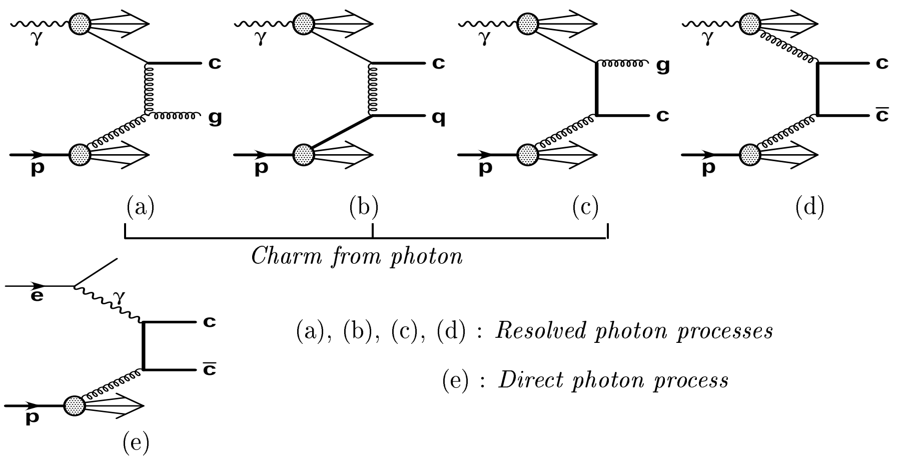

Fig. 1. Various sub-processes with charm, dominant in HERA region of phase space.

3.1. Measurement of $x_\gamma^{\rm obs}$

The variable $x_\gamma^{\rm obs}$, related to the momentum fraction of the parton from the photon, is defined as the fraction of the photon's energy participating in the production of the two highest transverse energy jets:

$$x_\gamma^{\rm obs} = \frac{\sum_{\rm jet1,2} E_{\rm T}^{\rm jet} {\rm e}^{-\eta^{\rm jet}}}{2yE_e}\,, \tag{1}$$

where yE_e is the initial photon energy. The normalised cross section as a function of $x_\gamma^{\rm obs}$ is shown in Fig. 2(a) compared with predictions from PYTHIA [3], HERWIG [4] and CASCADE [5]. As previously mentioned, the photon acts as a point like object for direct photon events, thus this momentum fraction ($x_\gamma^{\rm obs}$) is expected to be populated around high $x_\gamma^{\rm obs}$. The significant cross section at low $x_\gamma^{\rm obs}$ is consistent with the presence of resolved photon processes.

3.2. Dijet angular distribution in D^* photoproduction

The high and low $x_\gamma^{\rm obs}$ region were studied in more details in terms of dijet angular distribution, which are sensitive to the spin of the propagator. Fig. 2(b) shows the relative differential cross section as a funtion of $|\cos\theta^*|$, where θ^* is the angle between the jet-jet axis and the beam direction in the dijet rest frame. The distributions are enriched in direct photon ($x_\gamma^{\rm obs} > 0.75$) or resolved photon ($x_\gamma^{\rm obs} < 0.75$) events. The measured differential cross section $1/\sigma(\text{all } x_\gamma^{\rm obs})\ d\sigma/d|\cos\theta^*|$ for both of these

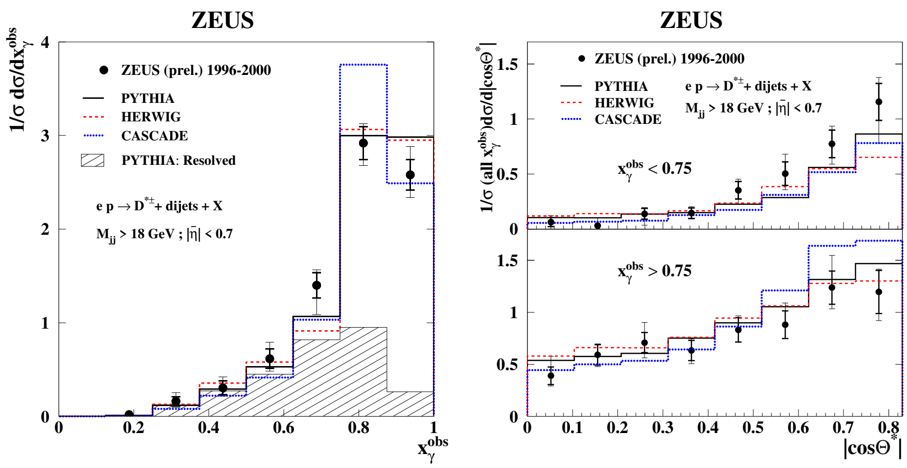

(a) (b)

Fig. 2. Relative differential cross sections $1/\sigma d\sigma/dx_{\gamma}^{\rm obs}$(left), $1/\sigma$(all $x_{\gamma}^{\rm obs}$) $d\sigma/d|\cos\theta^{*}|$(right) with $p_{\perp}^{D*} > 3$ GeV, $|\eta^{D*}| < 1.5$, $130 < W < 280$ GeV, $|\eta^{\rm jet1,2}| < 2.4$, $E_{\rm T}^{\rm jet1,2} > 5$ GeV, $M_{jj} > 18$ GeV and $|\overline{\eta}| < 0.7$. The results are compared with various MC simulations (histograms).

samples are significantly different, indicating that the dominant mechanism for direct photon like events proceed via $q-$exchange (spin$-1/2$ propagator, $\sigma \sim (1-\cos\theta^{*})^{-1}$), while resolved photon like events are dominated by $g-$exchange (spin-1 propagator, $\sigma \sim (1-|\cos\theta^{*}|)^{-2}$, as in Rutherford scattering).

Most of the partonic processes with at least one charm in the final state, which contribute in the lowest order, can be derived from Fig. 1 by including other diagrams that are related by crossing. Fig. 3(a) shows the matrix element distribution for such processes. As can be seen, the distributions that are symmetric in $\cos\theta^{*}$ are $\gamma g \to c\overline{c}$ and $gg \to c\overline{c}$; the other diagrams show asymmetry either in the photon(negative) or proton(positive) hemisphere. In order to study this behaviour of the matrix elements, the charm-initiated jet, D^{*} jet, and the other jet were separated in $\eta - \phi$ space ($\triangle R_i \equiv \sqrt{(\phi_{{\rm jet}_i} - \phi_{D*})^2 + (\eta_{{\rm jet}i} - \eta_{D*})^2}$; with D^{*} jet having the smallest $\triangle {\rm R}_{i(i=1,2)} < 1.0$). Thus the sign of the unfolded $\cos\theta^{*}$ distribution is given by the direction of the D^{*} meson (positive for proton direction).

Fig. 3(b) shows the differential cross-section $1/\sigma$(all $x_{\gamma}^{\rm obs}$) $d\sigma/d\cos\theta^{*}$ for both direct and resolved enriched samples. The shaded areas for $x_{\gamma}^{\rm obs} < 0.75$ and $x_{\gamma}^{\rm obs} > 0.75$ are, respectively, the contamination of the genuine direct and resolved PYTHIA contributions. The resolved enriched events in the photon hemisphere exhibit a strong rise towards large negative $\cos\theta^*$ values, consistent with $g-$exchange diagrams as expected from the matrix element distribution Fig. 3(a). The only $g-$exchange diagrams with this topology come from $cg \to cg$ and $cq \to cq$ (Fig. 1(a), (b)), where c originates from the photon. On the other hand, in the proton hemisphere, a mild rise towards large positive $\cos\theta^*$ is observed, which is consistent with the q-exchange diagrams (Fig. 1(c)). These observations provide clear evidence that the bulk of the resolved photon contribution is due to the charm content of the photon, rather than to the more conventional resolved process $gg \to c\bar{c}$.

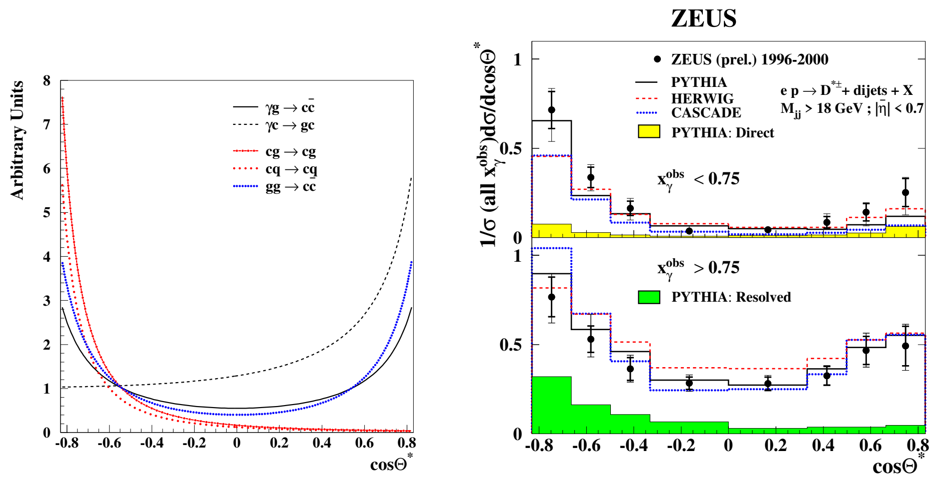

(a) (b)

Fig. 3. (a) The partonic cross section for $2 \to 2$ subprocesses, with at least a charm in the final state, as a function of $\cos\theta^*$; (b) Relative differential cross sections $1/\sigma(\text{all } x_\gamma^{\text{obs}})\ d\sigma/d\cos\theta^*$(right) in the same kinematic region as in Fig. 2. The shaded area for $x_\gamma^{\text{obs}} < 0.75(x_\gamma^{\text{obs}} > 0.75)$ plot is the contamination of the LO-direct (LO-resolved) photon contribution.

The direct enriched events are consistent with $\gamma g \to c\bar{c}$ (Fig. 1(e)). The slight asymmetry in the $x_\gamma^{\text{obs}} > 0.75$ distribution can be accounted for by the contamination from genuine resolved events, as given by PYTHIA.

4. Conclusions

The measurement of P_v is consistent with the universality of the charm fragmentation. Dijet angular distributions provide an important tool for understanding the heavy quark production and dynamics of underlying subprocesses. The $\cos\theta^*$ distribution for dijet events with a D^* shows a clear signature of gluon propagator for events with $x_\gamma^{\rm obs} < 0.75$, suggesting strong evidence that they mainly originate from the charm content of the photon.

REFERENCES

[1] ZEUS Collaboration, Study of Inclusive D^0 Photoproduction at HERA, paper 501, EPS HEP01, Budapest, Hungary, July 12-18, 2001.

[2] OPAL Collaboration, K. Ackerstaff *et al.*, *Eur. Phys. J.* **C5**, 1 (1998); ALEPH Coll., R. Barate *et al*, *Eur. Phys. J.* **C16**, 597 (2000).

[3] T. Sjöstrand, *Comput. Phys. Commun.* **82**, 74 (1994).

[4] G. Marchesini *et al.*, *Comput. Phys. Commun.* **67**, 465 (1992).

[5] H. Jung, Unintegrated parton densities applied to heavy quark production in the CCFM approach, preprint `hep-ph/0109146`.